

# Microstructure and thermal conductivity of carbon/carbon composites made with different kinds of carbon fibers

CHEN Jie(陈洁), LONG Ying(龙莹), XIONG Xiang(熊翔), XIAO Peng(肖鹏)

State Key Laboratory of Powder Metallurgy (Central South University), Changsha 410083, China

© Central South University Press and Springer-Verlag Berlin Heidelberg 2012

**Abstract:** The microstructure and surface state of three kinds of polyacrylonitrile-based carbon fibers (T700, T300 and M40) before and after high temperature treatment were investigated. Also, the pyrocarbon and thermal conductivity of carbon/carbon composites with different carbon fibers as preform were studied. The results show that M40 carbon fiber has the largest crystallite size and the least  $d_{002}$ , T300 follows, and T700 the third. With the increase of heat treatment temperature, the surface state and crystal size of carbon fibers change correspondingly. M40 carbon fiber exhibits the best graphitization property, followed by T300 and then T700. The different microstructure and surface state of different carbon fibers lead to the different microstructures of pyrocarbon and then result in the different thermal conductivities of carbon/carbon composites. The carbon/carbon composite with M40 as preform has the best microstructure in pyrocarbon and the highest thermal conductivity.

**Key words:** carbon fiber; thermal conductivity; pyrocarbon

## 1 Introduction

Carbon/carbon composites (C/C composites, carbon fiber reinforced carbon matrix composite) are considered as the best candidate materials for thermal management systems, due to the excellent properties such as light weight, large strength, high thermal conductivity and high temperature stability [1–3]. With the tendency of electronic equipments in aerospace crafts to miniaturization, lightweight and integration, heat dissipation has become the key for aeronautical materials [4].

Carbon fiber is the reinforcement in C/C composites which makes important contributions to thermal conduction of the composites. Therefore, the species and microstructure of carbon fibers have great influence on the thermal property (TC) of C/C composites. The polyacrylonitrile (PAN)-based carbon fiber is a polycrystalline material composed of amorphous carbon and graphite [5–7]. Different kinds of PAN-based carbon fibers have different surface states and different microstructures due to their different processing conditions. In the present work, the surface state and microstructure of three kinds of PAN-based carbon fibers before and after high temperature treatment (HTT) at different temperatures were investigated. And the pyrocarbon (PyC) microstructure and TC of C/C composites with different kinds of carbon fibers as preform were analyzed as well.

## 2 Experimental

### 2.1 Preparation of samples

Three kinds of PAN-based carbon fibers (T700, T300, M40) endured HTT at 2 000, 2 300 and 2 500 °C, respectively, for the investigations of carbon fibers. Three unidirectional preforms made from each kind of carbon fibers were prepared, with the same fiber content of 31%. After HTT at 2 000 °C for preforms, chemical vapor infiltration (CVI) was applied to densify the preforms to obtain C/C composites with the desired density at about 900 °C with propylene as carbon source. After CVI, the densified C/C composites went through final HTT at 2 300 °C.

### 2.2 Characterization

The morphologies of samples were observed by JSM-5600LV scanning electron microscopy (SEM). The microstructure was analyzed using Rigaku-3014 X-ray diffraction analyzer and polarized light microscope (PLM). Data of diffraction peaks (002) were obtained and the graphitization and crystallite size were calculated. The morphology and microstructure of PyC were examined by polarized light microscopy.

The TC of the composite was calculated by

$$\lambda = 418.68 a c_p d \quad (1)$$

where  $a$  is the thermal diffusivity,  $c_p$  is the specific heat

and  $d$  is the density of the composite. Thermal diffusivity was measured by laser flash method on JR-1 type synthetical thermal tester. Parameter  $c_p$  is 0.171 J/(g·K) for general C/C composites. The size of specimens was  $d10\text{ mm}\times 4\text{ mm}$ . Parallel TC refers to TC in the direction parallel to fiber axis and perpendicular TC refers to TC in the direction perpendicular to fiber axis.

### 3 Results and discussion

#### 3.1 Carbon fibers

The PAN-based carbon fiber has 2-D turbostratic

graphite crystal structure with the prior orientation along the direction of fiber axis [8–10]. Due to the different processing conditions, different kinds of carbon fibers have different properties and surface states.

Figure 1 shows the SEM micrographs of three kinds of fibers after HTT at different temperatures. It can be seen from Fig. 1 that the surface of T700 carbon fiber is smooth with few grooves and the surface state of fibers hardly changes after HTT at different temperatures. For T300 carbon fiber, shallow grooves and scratches along the direction of fiber axis appear after HTT at 2 000 °C and deepen with the increase of HTT temperature. As for

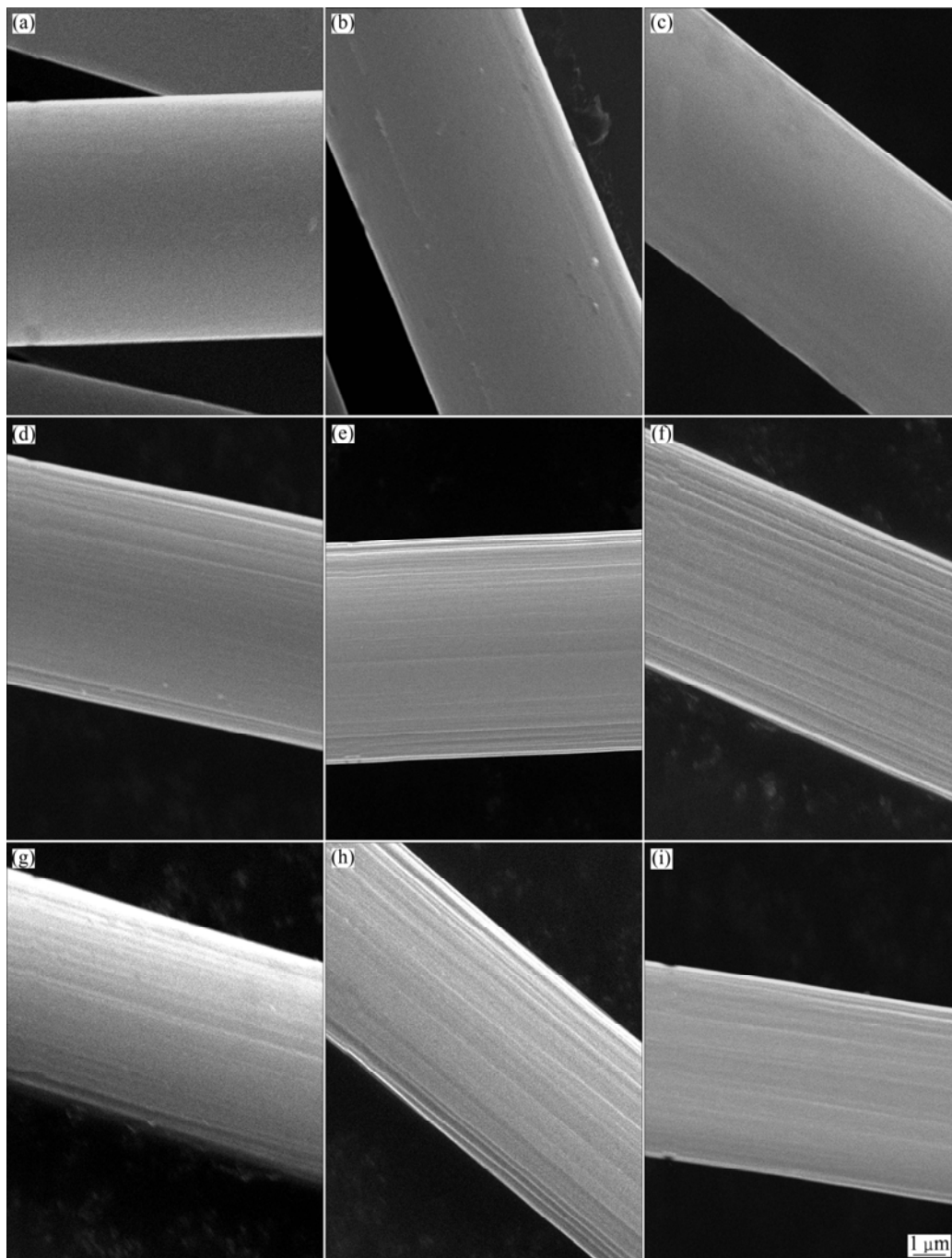


**Fig. 1** SEM micrographs of carbon fibers after HTT at different temperatures: (a) T700, 2 000 °C; (b) T700, 2 300 °C; (c) T700, 2 500 °C; (d) T300, 2 000 °C; (e) T300, 2 300 °C; (f) T300, 2 500 °C; (g) M40, 2 000 °C; (h) M40, 2 300 °C; (i) M40, 2 500 °C

M40 carbon fiber, there are also shallow grooves and scratches on its surface after HTT at 2 000 °C, but the grooves and scratches deepen seriously after HTT at 2 300 °C and then hardly change after HTT at 2 500 °C. It is obvious that the surface structure of carbon fibers has certain changes after HTT at different temperatures. The graphitization and crystallite size of carbon fibers before and after HTT at different temperatures are listed in Table 1.

**Table 1** Graphitization and crystallite size of carbon fibers before and after HTT

Carbon fiber	HTT temperature/°C	Crystallite size/nm	$d_{002}$ /nm	Graphitization/%
T700	Before HTT	2.3	0.3510	0
	2000	4.1	0.3455	0
	2300	4.7	0.3450	0
	2500	6.6	0.3436	14.4
T300	Before HTT	2.1	0.3515	0
	2000	4.7	0.3454	0
	2300	5.3	0.3446	3.3
	2500	6.2	0.3434	17.9
M40	Before HTT	2.5	0.3501	1
	2000	5.4	0.3447	6.5
	2300	5.4	0.3438	17
	2500	6.9	0.3423	30.7

With the increase of HTT temperature, the non-carbon compositions in carbon fibers volatilize out, and the microcrystallines deflect along the direction of fiber axis and grow up [11]. The degree of structural change with HTT is not the same for different kinds of carbon fibers.

By comparing T700 with T300, crystallite size of T300 increases and  $d_{002}$  of T300 decreases greatly with the increase of HTT temperature. There is few changes in T700, though T700 has larger crystallite size, less  $d_{002}$  than T300 before HTT (see Table 1). When HTT temperature reaches 2 300 °C, crystallite size of T300 is larger,  $d_{002}$  is less, and graphitization degree is higher than that of T700. We can also see from Fig. 1 that the surface of T300 carbon fiber changes obviously as the HTT temperature increases. Combining Table 1 and Fig. 1, as the temperature increases during HTT, the non-carbon elements in carbon fibers volatilize out from the surface of carbon fibers and the hexagonal microcrystal carbon layers deflect toward the direction of fiber axis, which results in the better arrangement of microcrystalline along the direction of fiber axis (the graphitization process). Therefore, the grooves and scratches along the direction of fiber axis are obvious on fiber surface. As the HTT temperature further increases,

in addition to the enhancement of microcrystalline orientation, the volatilization of non-carbon elements aggravates, so the grooves deepen in T300 carbon fiber. That is to say, T300 carbon fiber has stronger graphitization property than T700 carbon fiber during HTT.

For high-modulus carbon fiber M40, it has certain graphitization degree before HTT and has larger crystallite size, smaller  $d_{002}$  than the other two kinds of carbon fibers. Namely, the original M40 carbon fiber has large microcrystalline size, high orientation degree of hexagonal carbon layers along fiber axis and good closure of pores between carbon layers. The microcrystal structure of M40 changes greatly with the increase of HTT temperature. When HTT temperature gets to 2 300 °C, the graphitization degree and microcrystalline size of M40 are the same as those of T300 after HTT at 2 500 °C. As the HTT temperature reaches 2 500 °C, the graphitization degree of M40 reaches 30%, which indicates that M40 carbon fiber has high graphitizing ability with the increase of HTT temperature in addition to its original high graphitization.

### 3.2 Composites

Figure 2 shows the PLM micrographs of composites with different carbon fibers as preforms. In composite C-T700, PyC deposits surround the carbon fibers in shape of circular shell with homocentric annular cracks and clear cross extinctive stripe under PLM, which belongs to typical smooth layer (SL) PyC [12], as shown in Fig. 2(a). In composite C-T300, the PyC has higher optical anisotropy under PLM and less annular cracks compared with that of C-T700, as shown in Fig. 2(b). As for composite C-M40, PyC in it has distinct growing feature as well as high optical anisotropy under PLM, which is in somewhat concordance with rough layer (RL) structure described in Ref. [12]. And there are good interfaces between PyC and carbon fibers without obvious cracks in C-M40.

The microstructure of PyC deposited during CVI depends on the micro-environment in the course of CVI [13]. Generally, there are two kinds of reactions in CVI: gas–gas reaction and gas–solid reaction [14]. Three kinds of composites have the same preform structure and endure the same experiment process, so the micro-environments of gas–gas reaction in the three composites are basically identical. But, the surface of carbon fibers changes greatly after HTT, which leads to the distinct difference of surface state in different carbon fibers. Therefore, micro-environments for the deposition of carbon source gas on fiber surface are different in the three preforms. On the surface of carbon fibers, the grooves and scratches along the fiber axis can induce the

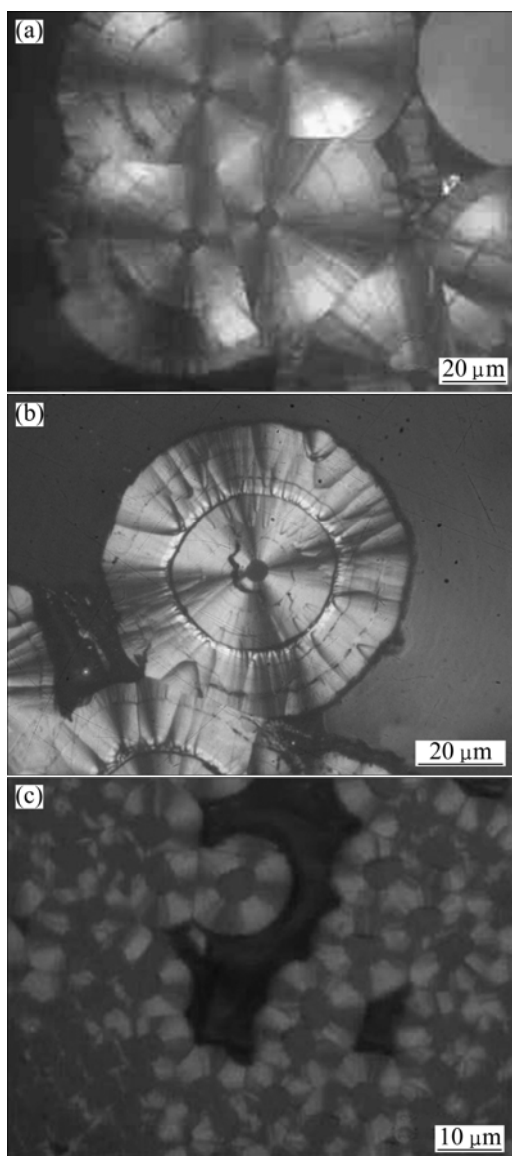


**Fig. 2** PLM micrographs of composites: (a) C-T700; (b) C-T300; (c) C-M40

ordered deposition of PyC around carbon fibers and then induce the better interface between carbon fiber and PyC. So, the PyC in C-M40 has the best microstructure and combines well with carbon fibers, PyC in C-T300 better, PyC in C-T700 the third.

The graphitization and thermal conductivity of composites are given in Table 2. Composite C-M40 has the highest graphitization degree and thermal

conductivity in both two directions, followed by C-T300 and then C-700.

As for C/C composites, the vibration of crystal lattices in carbon atoms is the base for heat conduction. The heat conduction in C/C composites may be regarded as the transfer of phonons in form of elastic waves. Namely, thermal conduction in C/C composites is the result of the interaction between phonons. According to Debby formula, thermal conductivity of C/C composites can be expressed as [15]

$$\lambda = (1/3)C \cdot v \cdot L \tag{2}$$

where  $L$  is the mean-free path (the distance that phonons propagate between two scatterings),  $C$  is the specific heat and  $v$  is the lattice vibration velocity. Thermal conductivity of carbon-graphite materials is mainly determined by the mean-free path ( $L$ ). Parameter  $L$  depends on the collision and scattering between phonons and is proportional to microcrystal size of material [16]. The working modes of phonons in C/C composites lie in: 1) phonon–phonon interaction, 2) phonon–imperfection or phonon–interface interaction.

Carbon fibers and carbon matrix are the main channels for heat conduction of C/C composites. Carbon fibers are the dominating heat transfer channel for thermal conductivity in the direction along fiber axis and carbon matrix is the primary heat transfer channel for thermal conduction in the direction perpendicular to fiber axis [17]. As for carbon fibers, M40 has the highest microstructure integrity, largest crystallite size and least  $d_{002}$ , T300 follows and then T700, according to Table 1. Thus, there are the highest phonon mean-free path and the lowest scattering centers in M40 carbon fiber, which leads to the effective heat conduction in it. As far as carbon matrixes are concerned, the PyC microstructures of three composites are different due to different surface states of the three carbon fibers. As mentioned above, PyC in C-M40 has the best preferential orientation of microcrystalline and least annular cracks. So, there are the highest phonon mean-free path and lowest scattering centers in the carbon matrix of C-M40, which does good to the thermal conduction of phonons. In summary, C-M40 has the highest thermal conductivity both in the parallel and perpendicular directions of fiber axis, C-T300 follows and then C-T700.

**Table 2** Properties of composites

Sample	Fiber content/%	Density/(g·cm <sup>-3</sup> )	Graphitization/%	Thermal conductivity/(W·m <sup>-1</sup> ·K <sup>-1</sup> )	
				Perpendicular direction	Parallel direction
C-T700	31	1.69	25	4.26	66.92
C-T300	31	1.68	28.6	7.21	82.76
C-M40	31	1.68	39.6	10.72	110.3

## 4 Conclusions

1) Among the three kinds of PAN-based carbon fibers T700, T300 and M40, M40 has the highest microcrystalline structure integrity, largest crystallite size and least  $d_{002}$ , T300 is the second and T700 is the third.

2) With the increase of HTT temperature, the surface and microstructure of carbon fibers change greatly. Some grooves and scratches along the direction of fiber axis appear after HTT. The graphitizing ability of M40 carbon fiber during HTT is best, T300 is the second and T700 is the worse.

3) The grooves and scratches along the direction of fiber axis on carbon fibers can induce the ordered deposition of PyC during CVI. The PyC structure of composite C-M40 is the best and the interface between carbon fibers and PyC combines well.

4) The composite with M40 carbon fiber as preform has highest thermal conductivity, the composite with T300 as preform follows and then the one with T700 as preform.

## References

- [1] BUCKLEY J D, EDIE D D. Carbon/carbon materials and composites [M]. New Jersey: Noyes Publications, 1993: 1–17.
- [2] LUO R Y. Current status of research and application of C/C composites used for aeroplane brake and engine [J]. Carbon Techniques, 2001, 4: 27–29. (in Chinese)
- [3] TORSTEN W, GORDON B. Carbon-carbon: A summary of recent developments and applications [J]. Materials & Design, 1997, 18: 11–15.
- [4] GAO X Q, GUO Q G, LIU L. The study progress on carbon materials with high thermal conductivity [J]. Journal of Functional Materials, 2006, 37: 173–177. (in Chinese)
- [5] CHAND S J. Carbon fibers for composites [J]. Mater Sci, 2000, 35: 1303–1013.
- [6] EDIE D D. The effect of processing on the structure and properties of carbon fibers [J]. Carbon, 1998, 36: 345–362.
- [7] LI D F, WANG H J, XUE L B. Preferred orientation of PAN-based carbon fibers during continuous graphitization [J]. Chemical Industry and Engineering Progress, 2006, 25: 1101–1109. (in Chinese)
- [8] HUNA. Y, YOUNG R.J. Effect of fiber microstructure upon the modulus of PAN-and pitch-based carbon fibers [J]. Carbon, 1995, 33: 97–107.
- [9] DATYE K V. PAN fiber variants [J]. Synth Fibers, 1997, 10: 5–10.
- [10] YING Y X, WO X Y. Review of carbon fiber's surface modification [J]. Spacecraft Recovery & Remote Sensing, 2004, 25: 51–54. (in Chinese)
- [11] LIU F J, WANG H J, FAN L D. The change of density under high temperature heat treatment in PAN-based carbon fibers [J]. New Chemical Materials, 2007, 35: 43–45. (in Chinese)
- [12] SUN W C, LI H J, HAN H M. Microstructure of the pyrocarbon matrix prepared by CLVI process [J]. Materials Science and Engineering, 2004, 369: 245–249.
- [13] XIONG J, ZOU Z Q, TANG Z H. Effect of carrier gas on the microstructure of CVI pyrocarbon in C/C composite [J]. Acta Materiae Compositae Sinica, 2004, 21: 87–92. (in Chinese)
- [14] XIONG X, TANG Z H, ZHANG H B. Effect of carrier gas on density and microstructure distribution of CVI-derived C/C composites [J]. The Chinese Journal of Nonferrous Metals, 2006, 16(3): 385–391. (in Chinese)
- [15] GUAN Z D, ZHANG Z T, JIAO J S. Physical performances of inorganic materials [M]. Beijing: Tsinghua University Press, 1992: 131–150. (in Chinese)
- [16] SAVAGE G. Carbon carbon composites [M]. London: Chapman & Hall, 1993: 309–317.
- [17] MANOCHA L M, WARRIER A, MANOCHA S. Thermophysical properties of densified pitch based carbon/carbon materials—I. Unidirectional composites [J]. Carbon, 2006, 44: 480–487.

(Edited by YANG Bing)